Relationship Between Particle Properties and Immunotoxicological Effects of Environmentally-Sourced Microplastics

Nick Beijer, Alexandre Dehaut, Maxim Carlier, Helen Wolter, Ron Versteegen, Jeroen Pennings, Liset de La Fonteyne, Helge Niemann, Henk Janssen, Belinda Timmermans, et al.

frontiers | Frontiers in Water

ORIGINAL RESEARCH
published: 31 May 2022
doi: 10.3389/frwa.2022.866732

Relationship Between Particle Properties and Immunotoxicological Effects of Environmentally-Sourced Microplastics

Nick R. M. Beijer[1], Alexandre Dehaut[2], Maxim P. Carlier[1], Helen Wolter[3], Ron M. Versteegen[4], Jeroen L. A. Pennings[1], Liset de la Fonteyne[1], Helge Niemann[3,5], Henk M. Janssen[4], Belinda G. Timmermans[1], Wim Mennes[1], Flemming R. Cassee[1,6], Marcel J. B. Mengelers[1], Linda A. Amaral-Zettler[3,7], Guillaume Duflos[2] and Yvonne C. M. Staal[1]*

[1] National Institute for Public Health and the Environment (RIVM), Bilthoven, Netherlands, [2] ANSES – Laboratoire de Sécurité des Aliments, Boulevard du Bassin Napoléon, Boulogne-sur-Mer, France, [3] Department of Marine Microbiology & Biogeochemistry, NIOZ Royal Netherlands Institute for Sea Research, Texel, Netherlands, [4] SyMO-Chem B.V., Eindhoven, Netherlands, [5] Department of Earth Sciences, Faculty of Geosciences, Utrecht University, Utrecht, Netherlands, [6] Institute for Risk Assessment Sciences, Utrecht University, Utrecht, Netherlands, [7] Department of Freshwater and Marine Ecology, Institute for Biodiversity and Ecosystem Dynamics, The University of Amsterdam, Amsterdam, Netherlands

OPEN ACCESS

Edited by:
Scott Coffin, California Water Resources Control Board, United States

Reviewed by:
Anja Franziska Ruth Marie Ramsperger, University of Bayreuth, Germany
Susanne Brander, Oregon State University, United States

***Correspondence:**
Nick R. M. Beijer
nick.beijer@rivm.nl

Specialty section:
This article was submitted to Water and Human Health, a section of the journal Frontiers in Water

Received: *31 January 2022*
Accepted: *18 April 2022*
Published: *31 May 2022*

Citation:
Beijer NRM, Dehaut A, Carlier MP, Wolter H, Versteegen RM, Pennings JLA, de la Fonteyne L, Niemann H, Janssen HM, Timmermans BG, Mennes W, Cassee FR, Mengelers MJB, Amaral-Zettler LA, Duflos G and Staal YCM (2022) Relationship Between Particle Properties and Immunotoxicological Effects of Environmentally-Sourced Microplastics. Front. Water 4:866732. doi: 10.3389/frwa.2022.866732

Background: Concerns on microplastics (MPs) in food are increasing because of our increased awareness of daily exposure and our knowledge gap on their potential adverse health effects. When particles are ingested, macrophages play an important role in scavenging them, potentially leading to an unwanted immune response. To elucidate the adverse effects of MPs on human health, insights in the immunotoxicity of MPs are essential.

Objectives: To assess the effect of environmentally collected ocean and land weathered MP particles on the immunological response of macrophages using a state-of-the art *in vitro* immunotoxicity assay specifically designed for measuring particle toxicity.

Methods: Environmentally-weathered macroplastic samples were collected from the North Pacific Subtropical Gyre and from the French coastal environment. Macroplastics were identified using (micro)Raman-spectrometry, FT-IR and Py-GC-MS and cryo-milled to obtain size-fractionated samples up to 300 μm. Physiochemical MP properties were characterized using phase contrast microscopy, gel-permeation chromatography, nuclear magnetic resonance, and differential scanning colorimetry. Macrophages (differentiated THP-1 cells) were exposed to particles (<300 μm) for 48 h before assessment of cell viability and cytokine release. Using both the physiochemical particle properties and biological data, we performed multi-dimensional data analysis to explore relationships between particle properties and immunotoxicological effects.

Results: We investigated land-derived polyethylene, polypropylene, polystyrene, and polyethylene terephthalate, water-derived polypropylene macroplastics, and virgin polyethylene fibers and nylon MPs. The different plastic polymeric compositions and MP size classes induced distinct cytokine responses. Macrophages had the largest response

to polyethylene terephthalate-particle exposure, including a dose-related increase in IL-1β, IL-8, and TNF-α secretion. Smaller MPs induced cytokine production at lower concentrations. Additionally, a relationship between both physical and chemical particle properties and the inflammatory response of macrophages was found.

Discussion: This research shows that MP exposure could lead to an inflammatory response *in vitro*, depending on MP material and size. Whether this implies a risk to human health needs to be further explored.

Keywords: microplastics, immune response, immunotoxicology, physiochemical characterization, macrophages, THP-1 cells, dose-response relationship

INTRODUCTION

Microplastics (MPs) are widespread anthropogenic contaminants that can be found in marine and fresh waters, the atmosphere, the urban environment, and even in food and beverages (Kontrick, 2018; Wayman and Niemann, 2021) including fish, shellfish, honey, sugar, beer, soft drinks, milk and tap and bottled drinking water (Kosuth et al., 2018; Kutralam-Muniasamy et al., 2020; Shruti et al., 2020). In 2020 MPs were defined for a California (USA) senate bill on MPs in drinking water. Here, MPs were defined as solid polymeric materials particles between 1 nm and 5 mm, which is significantly smaller than the MPs as defined 3 years earlier as plastic particles in sizes ranging from 1 micrometer up to 5 mm (Gigault et al., 2018). Evidence is growing for severe environmental contamination by these smaller particles as well – e.g., nanoplastics down to a size of 20 nm (Ter Halle et al., 2017; Lebreton et al., 2018; Wagner and Reemtsma, 2019). Ecotoxicological literature on the topic is growing, and recently, a human health focus is emerging. Humans may be exposed to MPs orally via ingestion, by inhalation of airborne particles or by absorption through dermal contact. Quantifying the extent of human exposure to micro- and nanoplastics (MNPs) is still in its infancy (Materić et al., 2020; Rubio et al., 2020; Mohamed Nor et al., 2021; Vethaak and Legler, 2021), which means that quantitative exposure data is limited.

Transport via water plays a significant role in introducing MP into the food chain (Cox et al., 2019). Intact plastic objects or fragmenting pieces of larger plastic - macroplastics - weathered on beaches and riverbanks - produce micro- and nanoplastics in the ocean and fresh water ecosystems (Wagner and Lambert, 2018). The most abundantly retrieved polymers as environmental contaminants are polyethylene (PE), polypropylene (PP), polystyrene (PS), polyvinyl chloride (PVC), polyurethane (PU), and polyethylene terephthalate (PET) (Geyer et al., 2017). These polymers come in a wide variety of shapes and often contain additives, such as plasticizers, flame-retardants, and pigments (Hermabessiere et al., 2017). In the environment, MPs are typically covered by complex biofilms comprised of microbial and microscopic life, as well as viruses and are surrounded by a protein corona (Zettler et al., 2013; Kirstein et al., 2016; Amaral-Zettler et al., 2020; Mughini-Gras et al., 2021; Vaksmaa et al., 2021).

Human exposure to MPs from the food chain occurs via the gastrointestinal tract after ingestion as highlighted by two recent studies reporting the presence of MPs in human stools (Schwabl et al., 2019; Zhang et al., 2021). Nonetheless very little is known about the distribution of micro- and nanoplastics in the human body and their ability to cross biological barriers (Paul-Pont et al., 2018). Smaller particles may be able to cross barriers more easily than larger particles, but properties other than particle size, such as particle chemistry, likely play a role as well (CONTAM., 2016; Schür et al., 2019; Kim et al., 2020), as does the shape of the MPs as e.g., particles or fibers (Dodson et al., 2020; González-Pleiter et al., 2020). Foreign particles in the intestines can be excreted via feces, but in addition, the absorbed particles can accumulate in the Peyer's patches. Here, macrophages encounter plastic particles as one of the first cells of the immune system and actively scavenge ingested particles (Boraschi et al., 2017). Their role in the first line of defense makes macrophages an important cell model to assess whether MP exposure may result in adverse effects. These adverse effects may result from the inability of macrophages to degrade engulfed particles, resulting in macrophage secretion of inflammatory cytokines. Screening of the effects of MP on inflammatory response by macrophages will contribute to the understanding of the potential impact of exposure to MPs on macrophages. The impact on macrophages can be designated as a key event in the mechanism resulting in an alteration of the functioning of the immune system, potentially leading to adverse effects on human health.

Contact with plastic material produces an inflammatory response. Strong macrophage-mediated immune effects, such as various (non-) immunological foreign body responses to polymer implant wear particles, have been observed in both human patients and animals already for decades (Goodman et al., 1994; Wooley et al., 2002; Vasconcelos et al., 2016; Wright and Kelly, 2017). More recently also information about the immunological responses of cells and organisms to MPs have been published (Hirt and Body-Malapel, 2020; González-Fernández and Cuesta, 2022; Weber et al., 2022). These reactions to polymer particles can be considered red flags when reflecting on the potential for similar effects induced by MPs.

Besides the potential induction of cellular toxicity by the chemical nature of polymers, there is a known role for additives, proteins and microorganisms on the surface of a MPs (Galloway, 2015), as well as physical particle properties (e.g., size). MPs

have sizes at which the physical material properties, e.g., stiffness, shape and surface structure, can affect cell behavior via various mechanotransduction routes (Kashiwada, 2006; Barboza et al., 2018; Leuning et al., 2018; Vassey et al., 2020). For example, high aspect ratio polymer fibers elicit a completely different cellular response than granular particles from the same type of polymer (Frère et al., 2018). Since particle properties may lead to adverse effects, it is important to characterize the particles used in toxicity tests as extensively as possible. Such information on particle properties is often lacking in articles studying MPs despite the fact that it is essential to relate particle properties to toxicological effects in the future.

Commercially available MPs have been shown to induce an inflammatory response in cells. PS particles of 44 nm diameter strongly enhanced the expression of Interleukin (IL)-6 and IL-8 in gastric adenocarcinoma cells *in vitro* at 1 to 10 μg/L (Forte et al., 2016). Minor acute toxicity was found for nanometer range PS particles at a wider concentration range of 0.01 mg/L and 100 mg/L (Hesler et al., 2019). Similar results on toxicity were obtained using 1, 4, and 10 μm PS particles at 60,000 to 250,000 particles/mL (Stock et al., 2019). Cytotoxicity has been found for small micrometer range PS and PE particles at the highest tested concentrations of 10 mg/L, possibly via an oxidative stress mechanism as quantified by increased reactive oxygen species (ROS) production (Schirinzi et al., 2017). As recently reviewed by Yong et al., the vast majority of published experiments on human cells used pristine MPs and not environmentally sourced secondary MPs (Yong et al., 2020). Depending on particle size and chemistry, cell type and whether or not the particles are taken up by cells, these studies only demonstrated a potential for low to moderate adverse effects on ROS production and pro-inflammatory responses at relatively high particle concentrations (Yong et al., 2020). Even though there are a significant number of studies on *in vivo* effects of MPs on marine life, there is clearly a lack of human *in vivo* data.

We aimed to elucidate the effect of environmentally collected ocean and land weathered MP particles (20–200 μm) on the immunological response of macrophages using an *in vitro* immunotoxicity assay specifically designed for measuring particle toxicity. Based on the size of the particles used, it is unlikely that the particles will be internalized by macrophages. However, interaction between macrophages and such particles may lead to a biological response. Particles were obtained by collecting plastic material from the environment, mill this into small particles and sieve to obtain size fractionated samples. Plastics were treated with hydrogen peroxide prior to exposure to remove biological material. As has been shown, any treatment and handling may affect properties such as particle surface or absorbed agents, which may lead to different biological effects (Rubin et al., 2021). As such, the particles in our experiments are environmentally sources but may not be environmentally realistic due to the treatment.

We hypothesized that the biological response, apart from the dose, depends on particle size and polymeric composition of MPs. Therefore, particle preparation and characterization was addressed in-depth to simulate the use of environmentally sourced particles, to develop potential reference materials, and to set a benchmark for particle characterization. Multiple modalities for in-depth characterization of the MPs physiochemical characteristics and multiple biological read-outs allowed us to perform clustering analysis and relate particle properties to immunological responses.

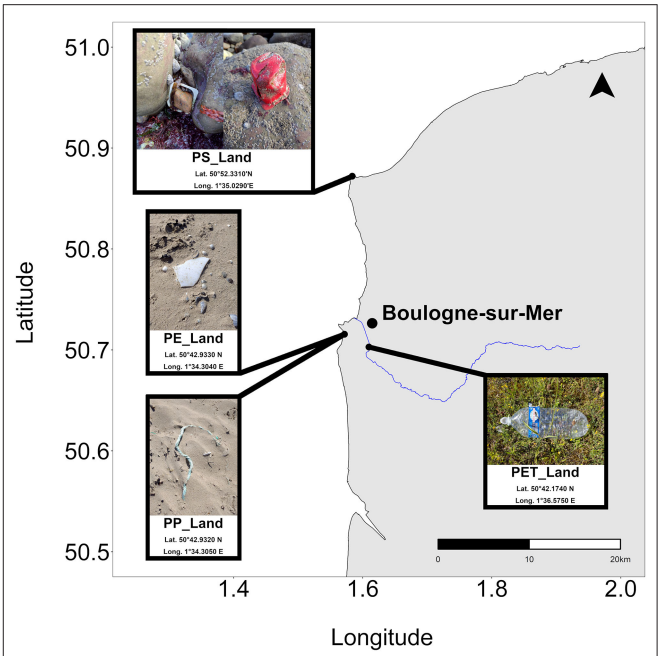

FIGURE 1 | Map with the locations of land-derived macroplastic collection. The scale bar illustrates a 20 km distance and the black arrow points North.

MATERIALS AND METHODS

(Micro)Plastic Sampling and Initial Identification and Processing

Terrestrial and Marine-Derived Plastics

Plastic litter was collected between June and August 2019 at different locations near Boulogne-sur-Mer (France). Four items were selected based on their diversity in appearance (**Figure 1**). Each sample was weighed before being processed and stored at −20°C.

The polymeric composition was determined upstream after the collection into the environment, e.g., before the washing step, on small pieces cut from harvested macroplastics using first pyrolysis coupled to gas chromatography and mass spectrometry (Py-GC/MS), then Raman microspectroscopy (μ-Raman) and finally Fourier transform Infrared spectroscopy (FT-IR). Protocols for Py-GC/MS and Raman analyses were adapted from previously published work (Hermabessiere et al., 2018). Here, Py-GC-MS samples were handled using an auto sampler (EGA/PY-3030D, Frontier Lab, Fukushima, Japan), all samples were analyzed with a GC2010-QP2010-Plus GC/MS (Shimadzu, Noisiel, France). All the interfaces from the pyrolyser to the ion source were set at 300°C. After pyrolysis at 700°C for 1 min, the pyrolysis products were injected with a split

of 10. Separation of the products was achieved on a RXi-5 ms® column (60 m, 0.25 mm, 25 μm thickness) (Restek, Lisses, France). The helium flow, oven program and mass parameters were kept constant. Finally, F-Search software 4.3 was used to identify the polymer from the total ion chromatogram (TIC) program. Identification was considered successful when similarity percentages reached 80% or higher, or when marker compounds were clearly highlighted. μ-Raman analyses were performed on a XploRA PLUS V1.2 (HORIBA Scientific, Palaiseau, France). Samples were analyzed with a laser at a wavelength of 785 nm. Time of acquisition was set at 2 s with 10 accumulation. Spectra were acquired from 200 to 3200 cm^{-1} with a 100x objective. Slit aperture and hole were respectively set at 200 and 500 μm. The polymer identification was carried out using the KnowItAll® spectroscopy software. Identification was considered as good where hit quality index was above 80. FT-IR analyses were performed on a Spotlight™ 400 FT-IR device equipped with a MCT. The micro attenuated total reflection automatic module equipped with a germanium crystal was used to perform measurements. All the spectra recorded were obtained using the same parameters, i.e : wavelength range from 4,000 to 600 cm^{-1}, with a resolution of 4 cm^{-1} and 25 accumulations. Measures were performed in the transmittance mode. Spectra were then compared to Flopp and Flopp-e databases (De Frond et al., 2021) and confirmed using the OpenSpecy database (Cowger et al., 2021). Identifications were validated when identification were higher than 0.7.

To generate MP samples from the collected macroplastics, the items were washed, ground and sieved. To avoid contamination of the cell culture, organic matter present on the surface of the plastics was removed using 0.22 μm filtered 30% (w/w) hydrogen peroxide solution (H_2O_2) (ref: 216763, Sigma-Aldrich, Saint-Quentin Fallavier, France). A ratio from 25 to 45 mL/g of 30% H_2O_2 was used to pre-treat the samples under a fume hood for 24 h at room temperature. Then samples were rinsed four times with 0.22 μm filtered analytical grade water (ref. 307586, Carlo Erba, Val-de-Reuil, France) under mild shaking for 5 min. Before grinding, the macroplastics were stored at −20°C.

For grinding, approximately 2.0 g of each macroplastic sample was placed in a stainless steel or polycarbonate tube. A milling piston was added and the two extremities were closed using two inox caps. Grinding was carried out using a Spex 6770 Freezer/Mill™ cryogrinder (Rickmansworth, UK), and cooled using liquid nitrogen. The protocol consisted of two cycles consisting of three steps: 2 min of cooling, 4 min of grinding at 15 cycles per second, and 2 min of post-milling cooling. For the collected samples, a set of 2 × 2 cycles was employed in order to collect a sufficient mass of the smallest particle fraction. Tube, caps, and piston were washed between samples using 70% ethanol and pressurized air.

Using inox sieves in combination with a Retsch AS 200 sieve shaker (30 min at 60 rpm) produced 20–50 μm, 50–100 μm, and 100–200 μm distinct size fractions. Samples were sieved as a powder (not suspended), resulting in possible adhesion of small micro-sized particles to bigger particles. Between sieving of the four sample types, sieves were washed using a specific four-step protocol: (1) vacuum cleaning of the inner, outer and join parts; (2) blowing with compressed air from the outer to the inner face; (3) rinsing outer, join and inner parts with 70% (v/v) ethanol; and, (4) blowing with compressed air from the outer to the inner face and join part.

Marine-Derived Plastics

Ocean-weathered plastics were sourced during a sampling campaign to the North Pacific Subtropical Gyre. The polymer composition was identified using Raman spectroscopy. Secondary MPs from macroplastics collected on the ship were generated, followed by dissolution and reprecipitation of the polymer (Davis et al., 2000; Hamad et al., 2013). In short, 1 g of each polymer was dissolved in 20 mL of organic solvent under constant stirring with a glass stirrer bar (PP in xylene/toluene (1/1 vol/vol) at 180°C for 60–90 min, and nylon 6,6 (Goodfellow GmbH, Polyamide-nylon 6,6 film, art.nr. AM321400) in trifluorethanol at 40°C for 30 min followed by the addition of 40 mL chloroform) and re-precipitated the solvent/polymer solution in anti-solvent (60 mL cold MilliQ for PP or 150 mL MilliQ for nylon) under constant stirring with a glass stirrer bar. The precipitated mixtures were vacuum filtered onto 0.7 μm glass fiber filters (Advantec, 47 mm) and dried at 65°C. After drying, the polymer was macerated with a ceramic mortar and pestle. Further, high density PE (HDPE) fibers were used as a virgin fiber particle [HDPE SHORT STUFF®miniFIBERS (MiniFIBERS Inc.: https://www.minifibers.com/)].

In-depth Chemical Characterization of the Generated Microplastics

Fourier Transform Infrared Spectroscopy

FTIR spectra were recorded in ATR mode on a Perkin Elmer 1600 FT-IR (UATR). MP samples were gently pressed on the ATR crystal (diamond), and the absorption of the infrared light in the range of 4000–450 cm^{-1} was measured. The spectra were compared to spectra from an online library of known FTIR polymer spectra (SDBSWeb: https://sdbs.db.aist.go.jp National Institute of Advanced Industrial Science and Technology, version 2018.07.18).

Differential Scanning Calorimetry

We used DSC to identify the melting point, melting enthalpy, and glass transition temperature of the particle materials. DSC was performed on a TA Instruments Q2000 DSC apparatus. For this, we prepared the samples for DSC analysis by weighing 5 – 10 mg of the MPs in the DSC sample pan. For determination of melting points and melting enthalpies, these samples were heated by 10°C per min from −80°C to 200 or 300°C (depending on the melting point of the MP) and subsequently cooled to −80°C at a similar rate. Additionally, glass transition temperatures were determined by heating at a rate of 40°C per min over the same temperature range.

Nuclear Magnetic Resonance Spectroscopy

We explored possibilities to perform polymer identification by ^{1}H-NMR on a Bruker Avance III HD (400 MHz for ^{1}H-NMR)

spectrometer (acquisition time: 4.0 sec, relaxation delay: 1.0 sec, spectral width: −2.0–14.0 ppm, number of scans: 64). However due to difficulties with the solubility in solvents suitable for NMR, not all samples could be analyzed. For PS we used chloroform-d1 as a solvent, for PET we used a 5:1 mixture of TFA-d1 and chloroform-d1, and for nylon we used pure TFA-d1. For the various PP and PE samples, we explored the use of chloroform-d1, DMSO-d6, THF-d8, para-xylene-d10, or TFA-d1 as possible solvents, either at room temperature or at elevated temperatures. However, using these solvents, we were not able to solubilize PP and PE particles sufficiently in order to prepare samples for NMR analysis.

Gel Permeation Chromatography

Gel permeation chromatography (GPC) was used to define the molecular weight of which the polymers of the MP particles were composed. GPC was measured on a Shimadzu Prominence-I LC-2030C 3D Liquid Chromatograph, using a Polymer Labs PLgel Mixed-C and -D column (5 μm 300 mm x 7.5 mm ID, MW-range 200 – 2,000,000 Da). Detection was done with a PDA detector at 254 nm. THF was used as the eluent for the PS samples. We prepared the GPC samples by dissolving MPs in THF at a concentration of 1 mg/mL, followed by filtration over a 0.2 μm PTFE filter. Number and weight-averaged molecular weights (Mn, resp. Mw) were calculated relative to polystyrene standards. This information can be used to compare particles which are weathered for different periods of time and possibly have shorter polymer chain lengths. Unfortunately, due to difficulties with the solubility of the other MPs in solvents suitable for GPC (e.g., chloroform, THF, DMF, or ODCB), these samples could not be analyzed, even at elevated temperatures.

Visualization and Size Quantification of Microplastics

The size distribution of the particles in each sample was determined by image analysis of photomicrographs. We created a 1,350 μg/mL suspension in cell culture media for each MP sample (polymer and size fraction). After vigorous vortexing, 100 μL of the suspension was transferred to a microplate well for microscopic analysis. Due to their density properties, PET and PS particles for all size fractions sunk in cell culture medium, whereas PE and PP particles floated. Therefore, PET and PS samples were imaged from the bottom of the microplate and PE and PP in the focal plane of the cell culture medium surface.

ImageJ 1.51n (NIH, Bethesda, USA) was used to analyze particle size. Based on the contrast between the MPs and the background signal, ImageJ identified the MPs as objects, allowing the measurement of the surface area (in μm^2) of the particles and their Feret diameter (in μm). Feret diameter is a measure for particle size based on the distance between two parallel lines on the outsides of a 2-dimensional projection of a 3-dimensional particle.

Cell Culture and Exposure Experiments

THP-1 Cell Culture

THP-1 cells (ATCC TIB-202) were cultured in RPMI 1,640 + L-glutamine (Gibco 11875093) cell culture medium, supplemented with 10% FBS (Gibco 10500064), and 1% penicillin/streptomycin (Gibco 15140122) at 37°C in a humidified environment and 5% CO_2. Before exposure to MPs, cells were differentiated to macrophages using phorbol 12-myristate 13-acetate (PMA) (Sigma Aldrich P1585). Cells ($5*10^4$ cells/well for sinking plastics or $10*10^4$ cells/well for floating plastics) were exposed to 100 ng/mL PMA in 96% ethanol for 3 h, after which the medium was replaced by fresh cell culture medium. After treatment, cells adhered to the bottom of typically used PS 96-well plates for exposure to sinking particles and to the basolateral side of microplate inserts (Costar 3470 and Costar 3413) for exposure to floating particles. Exposure to MPs started after an overnight settling period.

Exposure of THP-1 Cells to Microplastics

MP suspensions were created with concentrations of 1,350 μg/mL. This suspension was 1:3 diluted five times giving the following concentrations: 1,350, 450, 150, 50, 16.7, and 5.6 μg/mL. Directly after preparation, 120 μL of each dilution was added per 96-well plate well containing the differentiated THP-1 cells for 48 h of exposure. Nigericin [1.25 μM] and 100 ng/mL lipopolysaccharide (LPS) served as the positive control for inflammatory cytokine release, while cells cultured in basic cell culture medium acted as a negative control.

Cell Viability

WST-1 reagent (Roche 11644807001) was diluted 1:10 in cell culture media and incubated with the cell cultures for 1 h at 37°C. Subsequently, absorbance was measured at 440 nm using a SpectraMax M2 plate reader (Molecular Devices). WST-1 is a tetrazolium salt which is cleaved by mitochondrial dehydrogenase to formazan, and the amount of generated dye is directly proportional to the number of living cells.

Cytokine Release

After 48 h of exposure, cell culture supernatants were transferred to v-bottom 96-wells plates and stored at −80°C until processed further for ELISA analysis. We measured IL-1β (Invitrogen 88-7261-88), TNF-α (Invitrogen product 88-7346-88), IL-6 (Invitrogen 88-7066-88), IL-8 (Invitrogen 88-8086-88) and IL-10 (Invitrogen 88-7106-88) according to manufacturer instructions using a SpectraMax M2 plate reader (Molecular Devices).

PROAST Analysis for Dose-Responses

Dose-response analyses on the cytokine secretion data were performed using the European Food Safety Authority (EFSA) BMD webtool (EFSA Web Application for PROAST (version 69.0) available from: https://r4eu.efsa.europa.eu [accessed November 13, 2020]), which is based on the R-package PROAST version 69.0 (RIVM, Bilthoven, Netherlands). PROAST is a software package that fits dose-response curves for a given data set. Based on the dose-response curve fitting, the package calculates a confidence interval around a dose (benchmark dose - BMD) at which a predefined response (benchmark response - BMR) would occur. The lower (BMDL) and higher

(BMDU) bounds of this confidence interval (90% double sided) obtained after model averaging are conventionally described as BMDL and BMDU respectively. For the cytokine release data, a BMR of 0.2 was selected. This BMR of 0.2 represents a 20% change in cytokine production, which is in the steep part of the dose response curve meaning that comparisons are above background levels. Dose-response analysis of cytokine secretion was conducted to allow the comparison of effects between types of plastics and between particle sizes. Generally it is recommended to use a BMD of 10% to identify adverse effects (USEPA., 2012), however we decided to use a BMD of 20% for effects on cytokine secretion. A 20% increase in cytokine release was considered biologically relevant and beyond the variation in response that could be due to the variation in the assay. Most importantly as our aim was to compare the effects at the same level of response, and for such cases a clear response is more important than the identification of the lowest dose at which effects occurs. Subjecting the data to dose-response modeling using the EFSA webtool, we calculated both BMDL and BMDU limit around the BMD as a confidence interval of 90%. For this modeling, we used secretion data of IL-1β, TNF-α, and IL-8 after exposure to various polymers – both sinking and floating – and size fractions.

Statistical Analysis

Parameter Selection

For statistical analyses, we selected 19 parameters, based on their suitability for further interpretation (e.g., excluding FTIR spectra, and using the type of plastic instead), as well as having a sufficient number of data points for further analyses. Included parameters were classified as biological (IL-1β, IL-6, IL-8, TNF-α, WST-1), chemical (PE, PET, PS, PP, nylon, all as binary options), or physical (particles concentration, melting point, density (e.g., floating or sinking), size fractions, median diameter, percentages particles in the 0–20, 20–50, 50–100, and 100–200 μm ranges). Analyses were done in R version 4.0.0 or later.

Correlation Analyses

For each pair of parameters, we determined the Spearman correlation coefficient. Squared correlation coefficient (R^2) values were visualized as a heatmap combined with hierarchical clustering (1 - R^2 distance, Ward D linkage). Also, the 1 - R^2 distance matrix was used as input for multidimensional scaling (MDS) to obtain a visual overview of parameter relations.

Network Visualization

For visualization of parameter correlations, we reduced the set of all possible pairwise correlation coefficients to those that were: (1) supported by having mutual data in at least 40% of the data points (out of a total of 270); (2) significant at a False Discovery Rate-adjusted p-value < 0.05; (3) had an absolute R value of 0.25 or higher; and (4) were not a priori obvious, i.e. excluding negative correlations between different plastic types or between particle size range percentages. The resulting table was imported into Cytoscape 3.7.2. (Shannon et al., 2003) for network visualization.

Other Statistical Analyses

The particle size distribution was visualized using the polynomial fit function in MS Excel based on the number of particles within defined bins for particles sizes. Statistical significant differences between conditions was calculated using Non-parametric Kruskal-Wallis one-way ANOVA's in GraphPad Prism 8.4.1 (GraphPad Prism software Inc. San Diego, USA) and R version 3.6.0.

RESULTS

Macroplastic Polymer Identification and In-depth Molecular Microplastic Characterization

Upon macroplastic collection all items were successfully identified using a minimum of two out of the three identification techniques employed in this study. The four terrestrial-derived macroplastic items were identified as PET, PP, PE, and PS (**Table 1**), which is in line with the FT-IR identification of the subsequently generated MP samples (**Supplementary Figure 1**). Note, these generated MP samples will be designated as 'polymer type_Land'. The marine-derived macroplastic item was identified as PP using μ-Raman and FT-IR and designated as PP_Water from this point on. We also included virgin high-density PE (HDPE) fibers and nylon 6,6 as reference materials. Both materials were analyzed using μ-Raman and FT-IR and indeed identified as PE and nylon.

^{1}H-NMR analysis of PET, PS, and nylon samples confirmed their identification (**Supplementary Figure 2**). All three polystyrene size fractions gave similar ^{1}H-NMR-spectra, that were typical for atactic polystyrene. Where on the one hand all three-size fractions of each type of polymer were chemically similar, they exhibited differences in polymer chain length as determined by GPC-UV (**Table 2**). Unfortunately, due to low solubility of the PE and PP samples in solvents suitable for NMR, these samples could not be analyzed, even at elevated temperatures.

We also performed DSC to determine thermal properties and insights into crystallinity to further characterize the polymer configuration of the MP particles. From the DSC heat flow graphs (data not shown), we could extract melting point temperatures and melting enthalpies for all except the PS samples, and glass-transitions for PET, PS and nylon samples (**Table 3**). Furthermore, this provides insights into the extent to which the polymer morphology is crystalline or amorphous. We found: (1) similar melting point and enthalpy, and glass-transition temperature values for the three size fractions per polymer type; (2) two melting points for the polypropylene samples – indicating a polypropylene mixture existing of isotactic PP and an unknown form; (3) the polystyrene to be amorphous since no melting points and melting enthalpies were detected in these samples upon heating; and (4) due to the high crystallinity of PP and PE, no glass-transition temperatures could be detected for those samples. As stated in point 3 and 4, no values could be detected for those specific samples, which can be found in **Table 3** as "nd" – not detected.

TABLE 1 | Result of identification for the selected items, before transformation to microplastics.

Samples	Description	Identification[a,c,d]		
		Py-GC/MS	***μ-Raman***	***FT-IR***
PET_Land	Water plastic bottle	PET *(76%)*[b]	PET *(96.7%)*	PET *(98.8%)*
PE_Land	White piece of plastic	PE *(99%)*	PE *(76.8%)*	PE *(98.7%)*
PP_Land	Cordage	PP *(95%)*	PP *(90.4%)*	PP *(97.4%)*
PS_Land	Yogurt pot	PS *(93%)*	PS *(94.3%)*	PS *(98.4%)*
PP_Water			PP (>95%)	PP
PE_Fibers	HDPE SHORT STUFF®miniFIBERS		PE (>95%)	PE
Nylon_Virgin	Nylon 6,6 resin sheet		Nylon (>95%)	Nylon

[a] *Figures presented in italic between brackets corresponds to the identification scores obtained with the different techniques.*
[b] *Although inferior to 80%, the identification as PET has been validated, controlling specific peaks as presented in Hermabessiere et al. (2018).*
[c] *Scores obtained with Flopp-e database (De Frond et al., 2021).*
[d] *Scores obtained with Flopp database (De Frond et al., 2021).*

TABLE 2 | Gel permeation-chromatography measured molecular weights of polystyrene samples.

Samples	M_n (g/mol)	M_w (g/mol)	Polydispersity
PS_Land 20-50	84,800	214,500	2.5
PS_Land 50-100	95,900	231,700	2.4
PS_Land 100-200	103,100	246,200	2.4

Microplastics Size Characterization and Shape Visualization

To characterize the samples in terms of particle size distribution, we obtained a small sample out of the MP suspension for each type of polymer and size fraction, and imaged particles in one focal plane, e.g., at the bottom of a microwell for sinking, and at the medium surface for floating MPs (**Figure 2**). Since they were generated by cryomilling of macroplastics, the MPs as used in this study were irregular in shape, ranging from rod-shaped morphologies to spherical and highly irregular shapes. This visual inspection showed that the generated MPs have a strong similarity with the shapes of MPs as found in nature. The representative images in **Figure 2** show that we obtained clear differences in particle sizes between the fractions. However, along with the larger particles that were selected during the sieving procedure, smaller particles were found in the samples as well, due to the electrostatic clustering of smaller particles onto larger particles when handled as dry powder.

MP imaging using Scanning Electron Microscopy (SEM) allowed for better visualization of particle morphology. Due to highly similar particle morphologies between the various MP samples, we depicted representative SEM images of the three polystyrene samples at three different magnifications (**Supplementary Figure 3**). Again, it was clearly visible that particle size increases in the samples with larger size fractions. Furthermore, we observed a wide variety of particle shapes for particles as a whole as well as on a material surface structure level, strongly resembling a sub-section of microplastics as found in nature.

Using image analysis software (ImageJ version 1.53c) we measured the Feret diameter and surface area of each individual particle larger than 1 μm on the images (**Supplementary Figure 4**). We observed a significant difference in mean particle size within each sample. For PET_Land, PE_Land, and PS_Land, the increase in mean particle size was in line with the intended size fractionation. We next calculated the particle size distribution within each sample. Particle sizes were based on surface area, as this is an important dose metric for exposure of cells (Schmid and Stoeger, 2016). Particle size distribution was plotted relative to the total surface area. For this, particle areas in μm^2 of particles in one bin were added up and divided by the total surface in μm^2 of all particles. The resulting distributions show what percentage of the total particle-covered surface is covered by particles falling into each bin of the accompanying Feret diameters of those particles (**Figure 3**). For all polymers the defined size fractions have most of their weight in the aimed size range. Additionally, in the same sample, smaller and larger particles were present as well.

Exposure of THP-1 Cells to Microplastics

For the exposure experiments, we selected a concentration range up to the concentration of MPs at which the first signs of cytotoxicity occurred. In addition, the highest concentration was chosen so that the cell layer was not covered completely, as this will result in loss of viability due to reduced supply of nutrients and would also be seen as overload and unrealistic for the human situation. To gain insight into the toxicological effects of various MPs, we selected three different polymers PET_Land, PS_Land and Nylon_Virgin using the available size fraction for these MPs. For PET_Land 20–50, PET_Land 50–100, PS_Land 20–50, and Nylon_Virgin, we observed a significant increase in cytotoxicity, as measured using the metabolic marker WST-1, after 48 h of exposure at only the highest concentrations (**Supplementary Figure 5**). For PET_Land 100–200, PS_Land 50–100, and PS_Land 100–200, we did not observe a significant increase in cytotoxicity.

TABLE 3 | DSC-derived thermal properties.

Polymer	Size fraction (μm)	Melting point (°C)*	Melting enthalpy (J/g)*	Glass-transition temperature (°C)**
PET_Land	20–50	249	40.1	78
PET_Land	50–100	248	44.6	63
PET_Land	100–200	248	45.5	66
PE_Land	20–50	128	180.7	nd
PE_Land	50–100	128	180.3	nd
PE_Land	100–200	129	184.6	nd
PP_Land	20–50	131/165	41.6/56.7	nd
PP_Land	50–100	132/166	40.8/56.4	nd
PP_Land	100–200	132/165	41.3/59.6	nd
PS_Land	20–50	nd	nd	86
PS_Land	50–100	nd	nd	92
PS_Land	100–200	nd	nd	85
PP_Water	<300	157	76.7	nd
PE_Fibers	<300	129	182	nd
Nylon_Virgin	<300	258	68.6	64

For all samples, the heat flow was measured in heating and cooling cycles. From the heating runs, melting point and melting enthalpy, and glass transition temperature data were derived.
**Scanning rate 10°C/min.*
***Scanning rate 40°C/min.*
nd stands for not determined.

Based on the cell viability results, maximum concentrations of 1,350 μg/mL were used to expose THP-1 cells for 48 h to all MP samples, including the sinking and buoyant MPs of all size fractions. Regarding the release of IL-1β (**Figure 4**), TNF-α (**Supplementary Figure 6**), and IL-8 (**Supplementary Figure 7**) we found that: (1) exposure experiments with sinking particles were more robust in terms of repeatability and variance of data compared to exposure to floating particles; (2) the samples with the smallest particles (20-50 μm) gave the strongest response in cytokine secretion per unit mass; (3) for all polymers, the largest size fraction (100–200 μm) did not induce a significant increase in secretion of IL-1β, TNF-α, and IL-8; (4) both fibers and particles induced a response, which was not dependent on shape; (5) for the sinking particles we observed similar trends in secretion for all 3 cytokines; and (6) no significant effect was seen on IL-6 expression.

Dose-Response Analysis of the Cytokine Secretion Data

To further characterize the effect of MP exposure, the effect of MP particle size and material on cytokine release was further assessed using BMD analysis in which a 20% increase in cytokine release was considered a relevant effect (see Section PROAST Analysis for Dose-Responses). Sinking particles induced the most robust responses as seen in the narrow ranges between the BMDL and BMDU (IL-1β in **Figure 5**, TNF-α and IL-8 in **Supplementary Figure 8**). For all three cytokines, the response was higher for MPs in the smallest size range, whereas for the fraction with the largest particles an BMD could not be derived with certainty for cytokine levels. This directly indicates a size dependent effect on cytokine secretion of MPs. For the smaller fractions, we found a dose-dependent increase in cytokine secretion. Cytokine response was comparable for all plastic types, including BMDs per size fraction compared between the different types of polymer. Notably, the highest concentration used for exposure of Nylon_Virgin showed cytotoxicity and therefore cytokine responses are less reliable as part of a dose-response curve.

Interplay Between Chemical-Physical Particle Properties and Biological Responses

We applied a statistical multivariate approach to calculate, describe and visualize relationships between the physical and chemical particle properties and the biological responses as measured by both the cytokine secretion and cytotoxicity. For this, we used the following data as input: cytokine secretion (IL-1β, TNF-α, and IL-8), cytotoxicity (WST-1), particle polymeric composition, particle size distribution, density, concentration, and thermal properties. The fingerprint of variations per parameter over all samples allowed us to calculate the correlation between the individual parameters and cluster them based on similarity (**Figure 6A**). The combination of correlations were used to create a multidimensional scaling-plot in which the relations between all parameters could be investigated in a 2-dimensional plane (**Figure 6B**). Lastly, we created a network of all significantly correlating parameter pairs (FDR < 0.05, unadjusted $p < 0.035$, $|R| > 0.25$) and the interconnectivity between them (**Figure 6C**). From this, we were able to gain insight into the relationships between the physical and chemical parameters in relation to the biological responses. Here, we observed an influence of both the physical as well as the chemical parameters

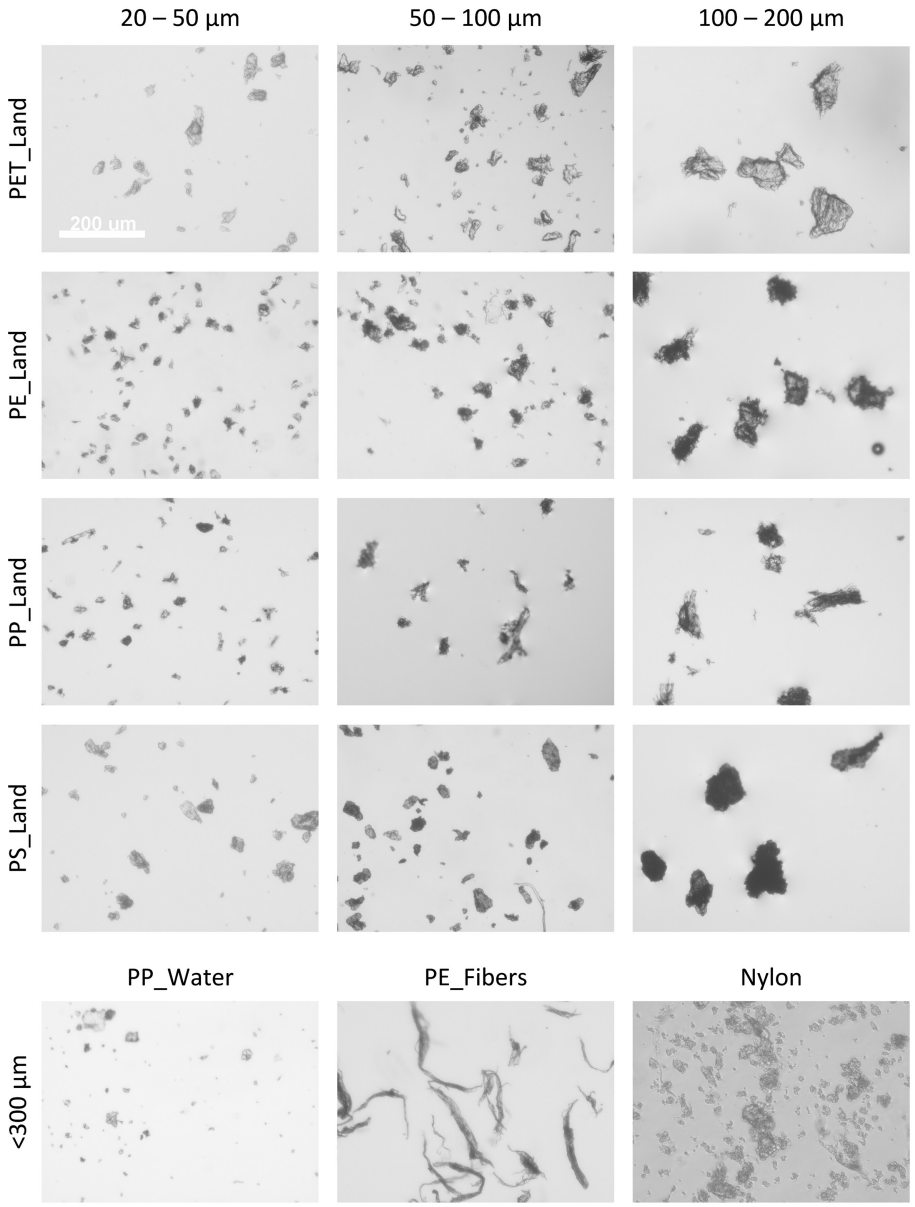

FIGURE 2 | Representative phase-contrast images of the various microplastic samples and size fractions. Images in grayscale, the white scalebar in the top-left image represents 200 µm and is applicable to all images in this figure.

on the biological response. More specifically, these results indicated that: (1) cytokine data are mutually related; (2) cytokine responses are mainly dependent on the concentration, and that (3) cytotoxicity depends more on particle size, with particularly the smaller particles (0–20 µm) contributing to the cytotoxicity; and, (4) thermal properties and density (e.g., floating/sinking properties) are less crucial for biological responses.

DISCUSSION

We have assessed the effect of environmentally collected ocean and land weathered MP particles (20–200 µm) on the immunological response of THP-1 derived macrophages, to gain understanding of the potential human health hazards of MPs. Our results show that the biological response is more pronounced for smaller particles (20–50 µm), however, the type of plastic plays a role as well. This work focused on the effects of MP on macrophages as a first indicator for an immunotoxicological response and it would be of interest to test this more in depth. In addition, it would be beneficial to include other toxicological end-points as well to determine the toxicological effects of MPs more completely.

To our knowledge, we are the first to present data of the immune-mediated effects of environmentally sourced plastics

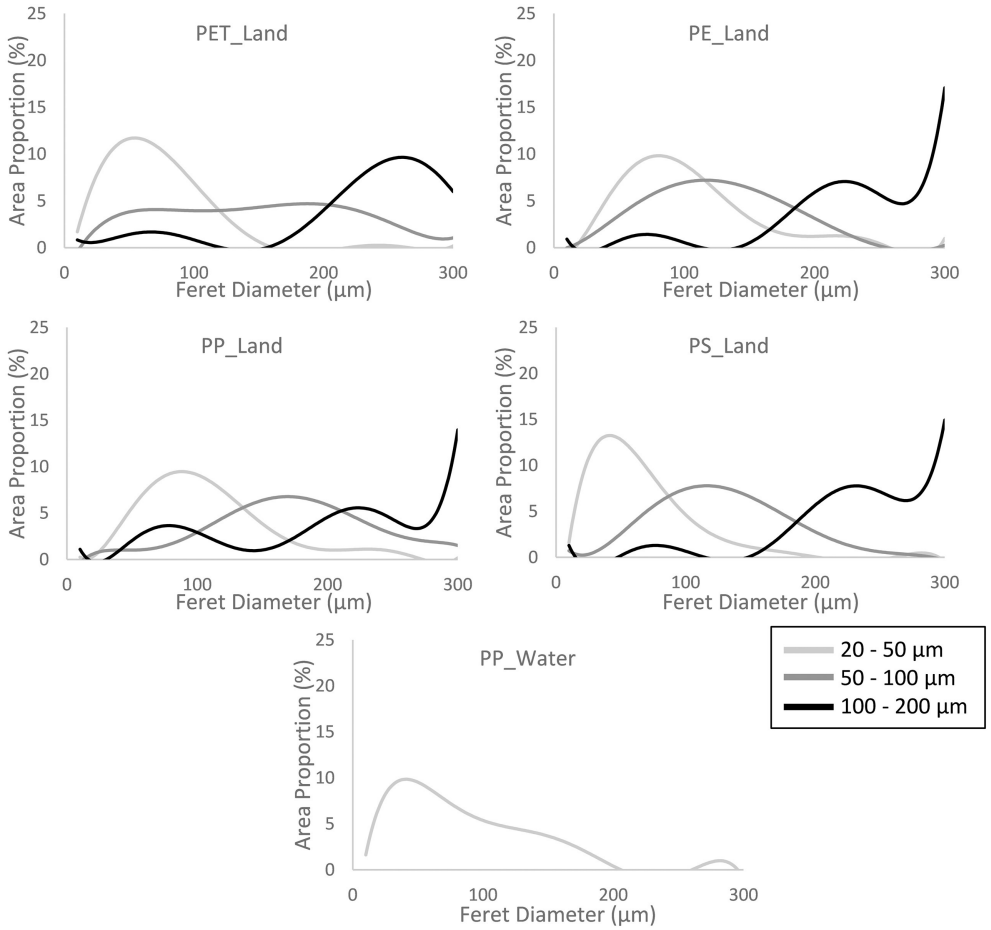

FIGURE 3 | Particle size distribution. The graphs represent the distribution of Feret diameters between 1 and 300 μm. The height of the curves represent the fraction of the sum of the 2-dimensional projection surface area of all particles within 1 bin (data divided in bins of 10 μm) relative to the sum of all particles measured per sample. The number of particles analyzed per sample ranged between 112 and 419. The sample PP_Water consist of 1 size fraction, namely <300 μm. See **Supplementary Table 1** for raw data.

on macrophages. Such data are important to assess the effects of MPs for human risk assessment. The effect of MPs on macrophage response has mainly been studied for spherical polystyrene particles. The effects of different types on plastics on hepatic and intestinal cells was assessed by Stock et al. (2021), who found material and size dependent effects (Stock et al., 2021). The ability of THP-1 derived macrophages to phagocytose plastic particles has been demonstrated although no effect on cytokine production was observed for 100,000 (1 μm), 250,000 (4 μm) or 60,000 (10 μm) particles per mL (Stock et al., 2019). The particles used in our studies are substantially larger and could therefore not be phagocytosed by THP-1 cells. Others have shown that amine-modified polystyrene nanobeads of 50 nm did induce IL-1β production in THP-1 macrophages at concentrations of 5–10 μg/cm^2, whereas no such effect was found for polystyrene or polyvinyl chloride nanobeads of similar sizes. In addition it would be beneficial to harmonize dosimetry to allow comparison of data (Busch et al., 2021). The concentrations in our experiments correspond between 2.1 μg/cm^2 (5.6 μg/mL) and 506 μg/cm^2 (1,350 μg/mL), which means that our results are in accordance with those found by Busch et al. (2021).

Previous studies with spherical PS particles gave indications of an effect, but as known from nanomaterial toxicology, particle properties play an important role in their toxicity (Gigault et al., 2021). Therefore, the assessment of effects of environmentally sourced particles, as used in our experiments, is needed to gain insight into the toxicity of MPs. Our experimental results allow assessment of the effects of different polymers and also of different particle sizes. The number of particles, which is higher for the smallest particles at similar mass concentration, their fate, as well as the expected effects are all related to the size of the particles (Vethaak and Legler, 2021). The size classes we have used in these experiments are among the particle sizes to which humans can be expected to be exposed to (Zhang et al., 2021). However, as we found a higher cytokine response for smaller particles, it seems likely that particles below the size range we have used, will induce a more pronounced biological response *in vivo*. More so, since the majority of the

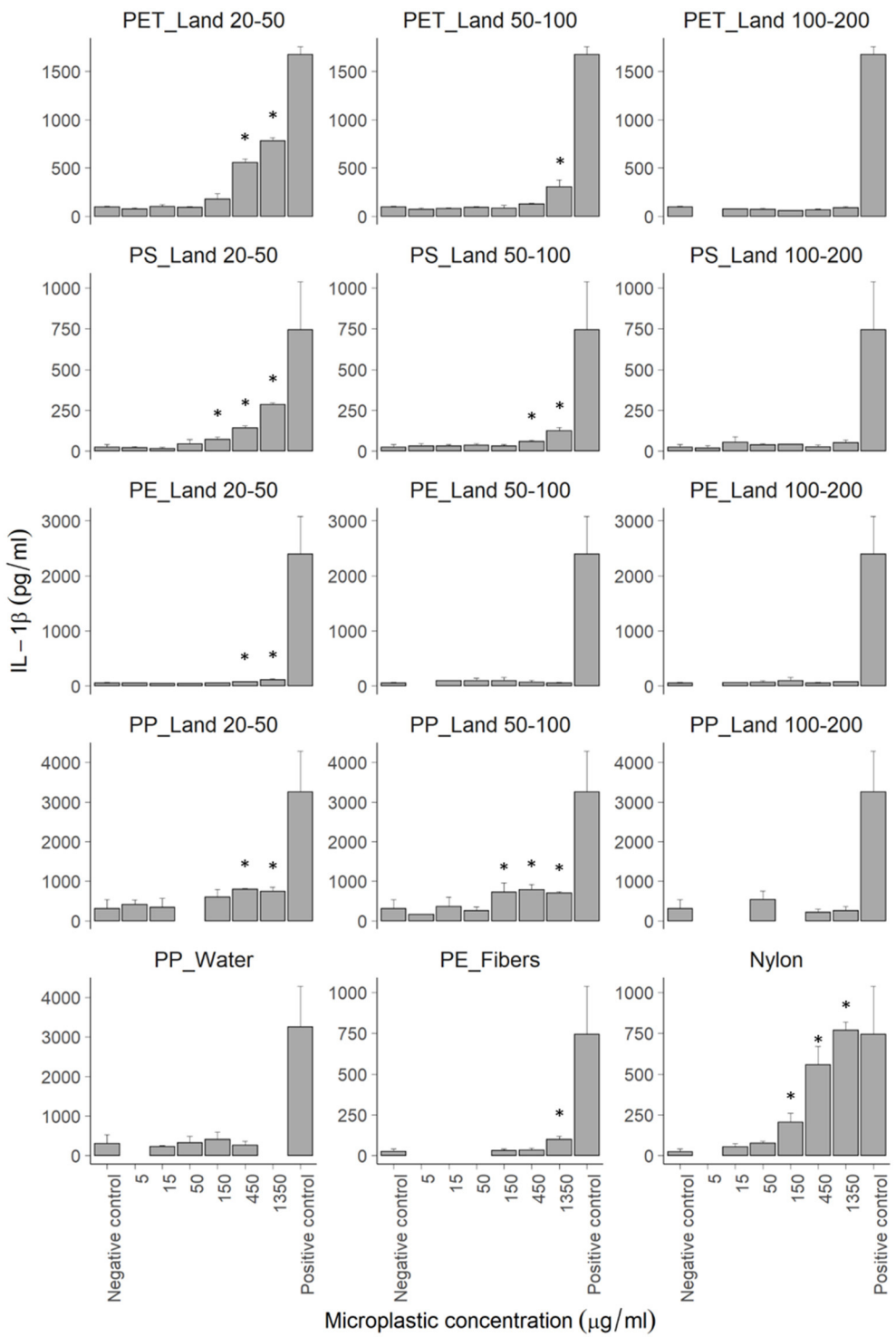

FIGURE 4 | IL-1β secretion by THP-1 cells after 48 h of exposure to various microplastic samples measured by ELISA. Bars represent the mean values (N > 3) with error bars to indicate the confidence interval at 95%. Positive controls were exposed to 1.25 μM Nigericin. Statistical significance indicated by stars with the following p-values: $^*P \leq 0.05$ as calculated using Non-parametric Kruskal-Wallis one-way ANOVA's.

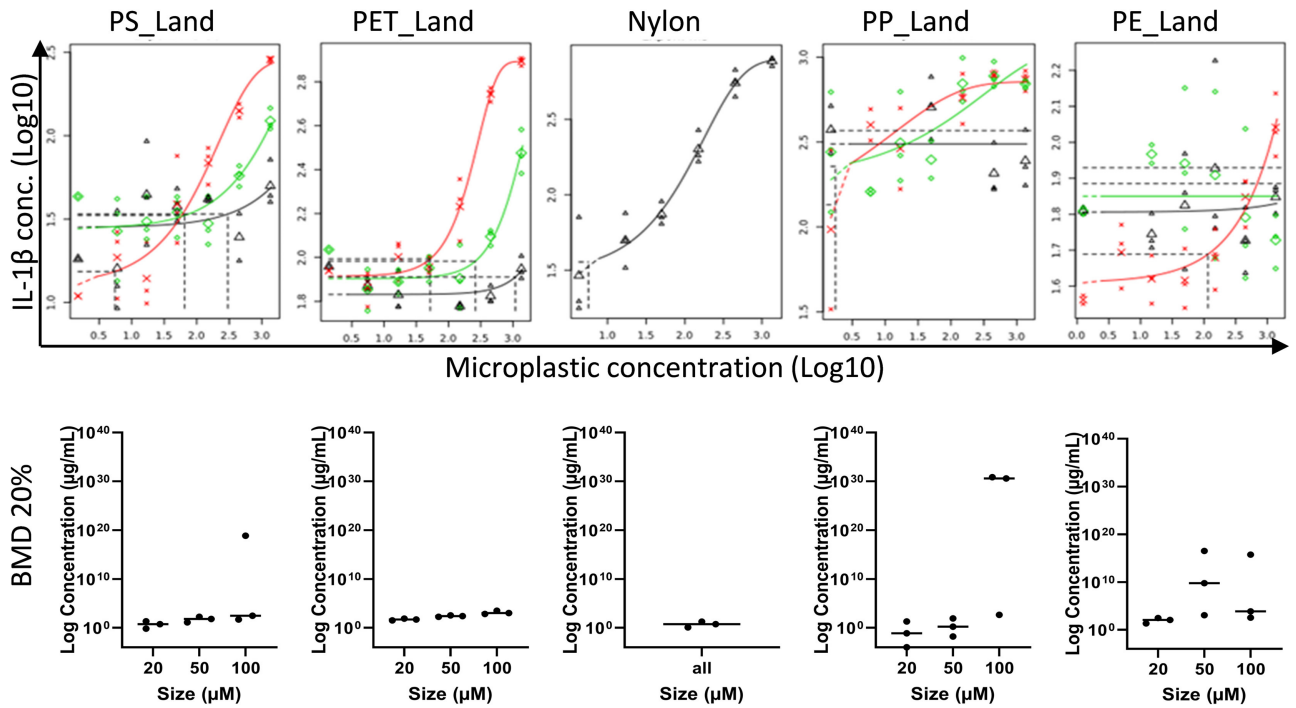

FIGURE 5 | Dose-response curves for IL-1β. Top row are the PROAST analysis on effects of exposure to PS_Land, PET_Land, nylon, PP_Land, and PE_Land. The red, green and black curves represent the dose-response curves for exposure to 20–50 µm, 50–100 µm and 100–200 µm respectively. For nylon only one size (<300 µm) was investigated (black). The dotted vertical lines indicate the microplastic concentration at which cytokines are increased by 20% compared to non-exposed macrophages. Bottom row shows the BMD analysis on effects of exposure to again PS_Land, PET_Land, nylon, PP_Land, and PE_Land. Size fractions are given on the X-axis (20–50 µm, 50–100 µm and 100–200 µm). BMD values are given on the Y-axis in log concentration, of which BMDL corresponds to the lowest dot, BMD the middle dot (vertical line), and BMDU the highest dot.

particles used in our experiments are too large to be engulfed by macrophages (Stock et al., 2021). Nevertheless, our results show that even when particles are not engulfed, they may lead to a macrophage response.

To our knowledge, we are the first to describe exposure of cells to floating particles. Exposure of cells to sinking particles is straight-forward, but studying floating particles comes with some technical challenges. By culturing the cells on the basolateral side of a cell culture insert, contact between the floating MPs in cell culture medium and the cells could be established. Biological responses of floating particles were more variable compared to exposures with sinking particles. As THP-1 cells only attach after differentiation, the yield of differentiation determines the number of cells able to attach to the insert. Differences in number of cells did, however, not explain the variation in the experiment. For both sinking and floating particles it is important to keep in mind that contact between cells and particles is dependent on the fraction of the particles which comes into contact with the cells. Particles that stay in suspension will not be in contact with the cells and can therefore not cause a biological effect directly.

Our results indicate that size-fraction, concentration, and polymer type are the most important determinants for the biological response, which in our experiments was based on cytokine secretion. This is supported by earlier findings on hepatic and intestinal cells (Stock et al., 2021). Inclusion of materials with different properties, such as different precisely defined shapes, and of various chemical compositions would allow for further linking of MP properties to biological effect. Characterization of immunological effects could be further extended to phagocytosis of MPs, which is a functional read-out for clearance capacity of macrophages. Inclusion of different exposure durations in contrast to the single exposure duration in these experiments, would allow assessment of MP effects and phagocytosis over time. Addition of additional assays for other end-points, not limited to immunological responses, would even further improve the network, which contributes to determining the properties of MPs that are contributors to biological response. Such information can ultimately be used for risk management and for policy makers to define modes of action for securing public health.

To avoid contamination of our cell culture, we have treated the particles with hydrogen peroxide to remove biological material. In real life particle exposure, such biological material remains on the particles and may also induce biological effects (Hirt and Body-Malapel, 2020). For future research we therefor recommend to include particles with and without the biological material, which allows discrimination of particle and biological effects. We aimed to compare the effects of MPs of different

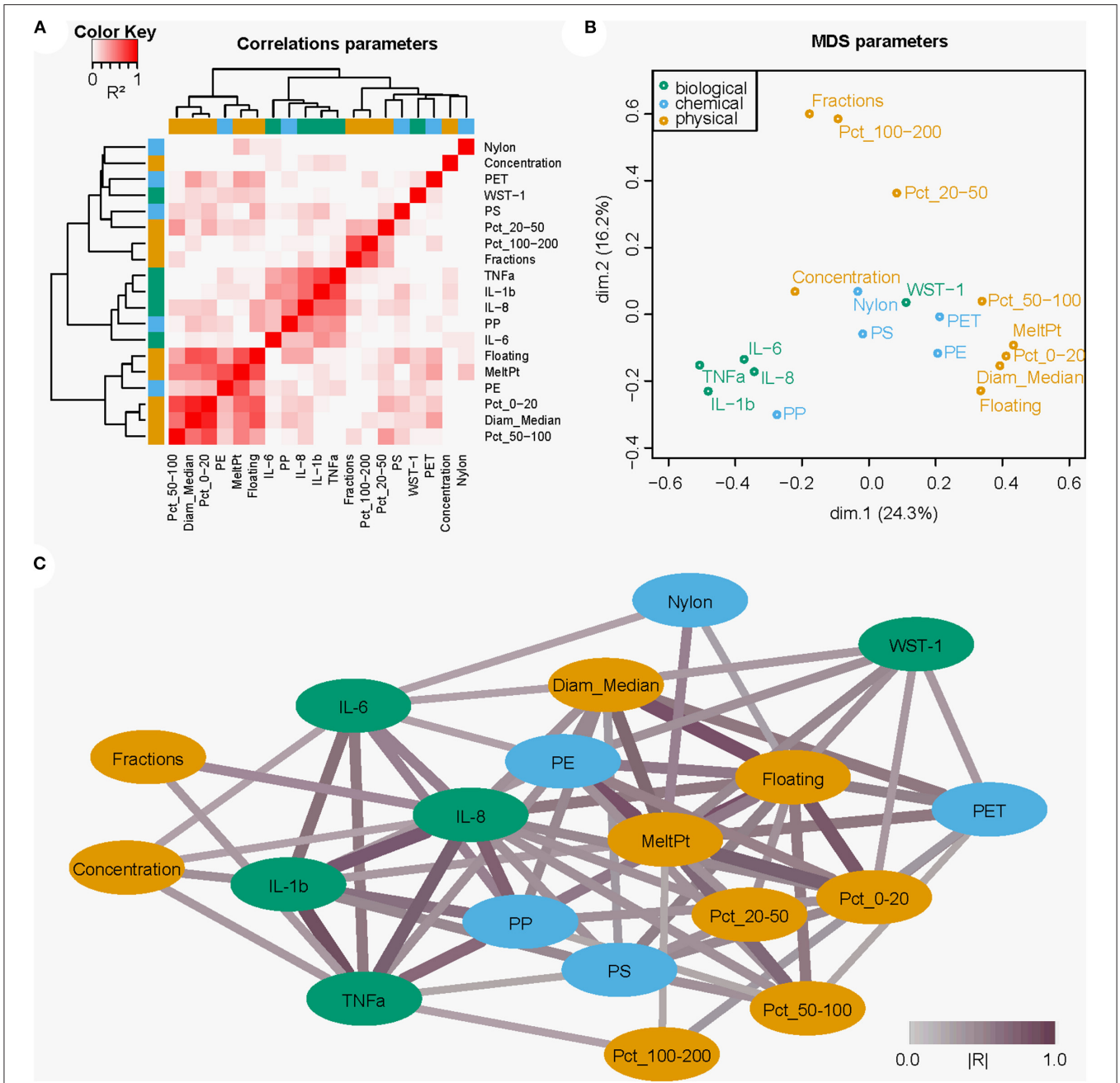

FIGURE 6 | Multivariate and network analysis approach visualizing the relationships between the chemical and physical particle properties and biological responses of THP-1 cells to the microplastic samples. **(A)** Heatmap showing correlations (R2) between selected parameters and clustering of the parameters on similarity. **(B)** Multidimensional scaling showing (dis)similarities (based on the calculated correlations) as distances between the parameters. **(C)** Cytoscape network analysis showing significant parameter correlations as network connections. Line color indicates correlation strength, with deeper shades of purple indicating higher |R| values. In orange the physical parameters, blue chemical, and green biological.

chemical and physical composition to ultimately determine MP properties that influence a biological response. As differences between equipment and assays are common, the use of a reference material can help to explain the differences in results between labs. As such reference material is not available for MPs yet, proper characterization of particle properties is crucial. We have included extensive particle characterization, but, despite the efforts made, some data could not be produced due to the lack of accurate methods. Particle characterization could be improved by information on the additive or non-intentionally added

substances (NIAS) composition. Paul-Pont et al. (2018) described constraints and priorities for MPs exposure. Standardization of materials and methods employed for exposure and particle characterization to ensure data quality has been proposed for ecotoxicity testing but can be applied for human toxicity testing as well (Koelmans et al., 2019; Mohamed Nor et al., 2021).

Our experiments have focused on the determination of a human health hazard in relation to particle properties, not necessarily to determine a human health risk. To be able to conclude whether MPs pose a risk to human health, information on exposure should be considered. Additionally, information is needed on ingestion of MPs and resulting bioavailability in the other target tissues. As a next step, hazard assessment of MPs at these target tissues can be assessed. To put our results into this perspective, we roughly estimate that our cells were exposed to a concentration range of 30–7,000 particles per insert of 0.32 cm^2 for the smallest particle fraction. Assuming a human consumption of 40,000 MPs per year (Cox et al., 2019), which corresponds to 110 particles per day, our exposure levels are substantially higher than daily human exposure. The question remains however, whether this induction of cytokines results in adverse effects on the long term.

CONCLUSION

We have shown that MPs generated from macroplastic from land and sea via cryomilling, as well as commercially available virgin materials induce a dose-dependent cytokine response (in IL-1β, TNFα and IL-8) in differentiated THP-1 cells. The correlation of the physiochemical characteristics of the particles with the biological response showed that particle size more strongly correlated with biological responses than polymer type. Further research should elucidate whether stronger responses are found for even smaller particles and whether other cell-physiological and toxicological parameters may be affected by MP exposure. Such information would allow determination of relationships between physiochemical properties and biological effects, which can be used to characterize the possible toxicity of MPs.

DATA AVAILABILITY STATEMENT

The original contributions presented in the study are included in the article/**Supplementary Material**, further inquiries can be directed to the corresponding author/s.

AUTHOR CONTRIBUTIONS

NB, AD, RV, HN, HJ, FC, MM, LA-Z, GD, and YS: conception and design of the study. AD, MC, HW, RV, LF, and BT: laboratory experiments. JP, WM, and MM: dose-response and modeling. NB, AD, RV, JP, HN, HJ, MM, LA-Z, and YS: manuscript writing. All authors contributed to manuscript revision, read, and approved the submitted version.

FUNDING

This study has been financially supported by the ZonMw program Microplastics and Human Health Project number 458001005 awarded to NB, AD, HN, HJ, MM, LA-Z, GD, and YS, the European Union European Regional Development Fund (ERDF), the French State, the French Region Hauts-de-France and Ifremer, in the framework of the project CPER MARCO 2015-2020. HN additionally received funding through the European Research Council (ERC-CoG Grant No. 772923, project VORTEX).

ACKNOWLEDGMENTS

Authors are thankful to Dr. Fabienne Lagarde and Frederic Amiard for their valuable help in the grinding and sieving part of this work.

SUPPLEMENTARY MATERIAL

The Supplementary Material for this article can be found online at: https://www.frontiersin.org/articles/10.3389/frwa.2022.866732/full#supplementary-material

REFERENCES

Amaral-Zettler, L. A., Zettler, E. R., and Mincer, T. J. (2020). Ecology of the plastisphere. *Nat. Rev. Microbiol.* 18, 139–151. doi: 10.1038/s41579-019-0308-0

Barboza, L. G. A., Dick Vethaak, A., Lavorante, B., Lundebye, A. K., and Guilhermino, L. (2018). Marine microplastic debris: an emerging issue for food security, food safety and human health. *Mar. Pollut. Bull.* 133, 336–348. doi: 10.1016/j.marpolbul.2018.05.047

Boraschi, D., Italiani, P., Palomba, R., Decuzzi, P., Duschl, A., Fadeel, B., et al. (2017). Nanoparticles and innate immunity: New perspectives on host defence. *Semin. Immunol.* 34, 33–51. doi: 10.1016/j.smim.2017.08.013

Busch, M., Bredeck, G., Kämpfer, A. A. M., and Schins, R. P. F. (2021). Investigations of acute effects of polystyrene and polyvinyl chloride micro- and nanoplastics in an advanced in vitro triple culture model of the healthy and inflamed intestine. *Environ. Res.* 193, 110536. doi: 10.1016/j.envres.2020.110536

CONTAM. (2016). Efsa panel on contaminants in the food chain: Statement on the presence of microplastics and nanoplastics in food, with particular focus on seafood. *EFSA J.* 14, 30. doi: 10.2903/j.efsa.2016.4501

Cowger, W., Steinmetz, Z., Gray, A., Munno, K., Lynch, J., Hapich, H., et al. (2021). Microplastic spectral classification needs an open source community: Open specy to the rescue! *Anal. Chem.* 93, 7543–7548. doi: 10.1021/acs.analchem.1c00123

Cox, K. D., Covernton, G. A., Davies, H. L., Dower, J. F., Juanes, F., and Dudas, S. E. (2019). Human consumption of microplastics. *Environ. Sci. Technol.* 53, 7068–7074. doi: 10.1021/acs.est.9b01517

Davis, R. D., Steadman, S. J., Jarrett, W. L., and Mathias, L. J. (2000). Solution 13c nmr characterization of nylon 66: Quantitation of cis amide conformers, acid and amine end groups, and cyclic unimers. *Macromolecules*. 33, 7088–7092. doi: 10.1021/ma000744x

De Frond, H., Rubinovitz, R., Rochman, C. M. (2021). ?atr-ftir spectral libraries of plastic particles (flopp and flopp-e) for the analysis of microplastics. *Anal Chem*. 93, 15878–15885. doi: 10.1021/acs.analchem.1c02549

Dodson, G. Z., Shotorban, A. K., Hatcher, P. G., Waggoner, D. C., Ghosal, S., and Noffke, N. (2020). Microplastic fragment and fiber contamination of beach sediments from selected sites in virginia and north carolina, USA. *Mar Pollut Bull*. 151, 110869. doi: 10.1016/j.marpolbul.2019.110869

Forte, M., Iachetta, G., Tussellino, M., Carotenuto, R., Prisco, M., De Falco, M., et al. (2016). Polystyrene nanoparticles internalization in human gastric adenocarcinoma cells. *Toxicol. In Vitro*. 31, 126–136. doi: 10.1016/j.tiv.2015.11.006

Frère, L., Maignien, L., Chalopin, M., Huvet, A., Rinnert, E., Morrison, H., et al. (2018). Microplastic bacterial communities in the bay of brest: Influence of polymer type and size. *Environ. Pollut*. 242, 614–625. doi: 10.1016/j.envpol.2018.07.023

Galloway, T. S. (2015). "Micro- and Nano-Plastics and Human Health" in *Marine Anthropogenic Litter*, eds Bergmann M, Gutow L, Klages M (Cham: Springer), 343–366.

Geyer, R., Jambeck, J. R., and Law, K. L. (2017). Production, use, and fate of all plastics ever made. *Sci. Adv*. 3, e1700782. doi: 10.1126/sciadv.1700782

Gigault, J., El Hadri, H., Nguyen, B., Grassl, B., Rowenczyk, L., Tufenkji, N., et al. (2021). Nanoplastics are neither microplastics nor engineered nanoparticles. *Nat. Nanotechnol*. 16, 501–507. doi: 10.1038/s41565-021-00886-4

Gigault, J., Halle, A.t, Baudrimont, M., Pascal, P.Y., Gauffre, F., Phi, T.L., et al. (2018). Current opinion: What is a nanoplastic? *Environ. Pollut*. 235, 1030–1034. doi: 10.1016/j.envpol.2018.01.024

González-Fernández, C., and Cuesta, A. (2022). Nanoplastics increase fish susceptibility to nodavirus infection and reduce antiviral immune responses. *Int. J. Mol. Sci.* 23, 1–12. doi: 10.3390/ijms23031483

González-Pleiter, M., Edo, C., Velázquez, D., Casero-Chamorro, M. C., Leganés, F., Quesada, A., et al. (2020). First detection of microplastics in the freshwater of an antarctic specially protected area. *Mar. Pollut. Bull.* 161, 111811. doi: 10.1016/j.marpolbul.2020.111811

Goodman, S., Wang, J. S., Regula, D., and Aspenberg, P. (1994). T-lymphocytes are not necessary for particulate polyethylene-induced macrophage recruitment. Histologic studies of the rat tibia. *Acta Orthop. Scand*. 65, 157–160. doi: 10.3109/17453679408995425

Hamad, K., Kaseem, M., and Deri, F. (2013). Recycling of waste from polymer materials: An overview of the recent works. *Polym. Degrad. Stabi*. 98, 2801–2812. doi: 10.1016/j.polymdegradstab.2013.09.025

Hermabessiere, L., Dehaut, A., Paul-Pont, I., Lacroix, C., Jezequel, R., Soudant, P., et al. (2017). Occurrence and effects of plastic additives on marine environments and organisms: a review. *Chemosphere*. 182, 781–793. doi: 10.1016/j.chemosphere.2017.05.096

Hermabessiere, L., Himber, C., Boricaud, B., Kazour, M., Amara, R., Cassone, A. L., et al. (2018). Optimization, performance, and application of a pyrolysis-gc/ms method for the identification of microplastics. *Anal. Bioanal. Chem*. 410, 6663–6676. doi: 10.1007/s00216-018-1279-0

Hesler, M., Aengenheister, L., Ellinger, B., Drexel, R., Straskraba, S., Jost, C., et al. (2019). Multi-endpoint toxicological assessment of polystyrene nano- and microparticles in different biological models in vitro. *Toxicol. In Vitro*. 61, 104610. doi: 10.1016/j.tiv.2019.104610

Hirt, N., and Body-Malapel, M. (2020). Immunotoxicity and intestinal effects of nano- and microplastics: a review of the literature. *Part Fibre Toxicol.* 17, 57. doi: 10.1186/s12989-020-00387-7

Kashiwada, S. (2006). Distribution of nanoparticles in the see-through medaka (oryzias latipes). *Environ. Health Perspect*. 114, 1697–1702. doi: 10.1289/ehp.9209

Kim, J., Poirier, D. G., Helm, P. A., Bayoumi, M., Rochman, C. M. (2020). No evidence of spherical microplastics (10–300 μm) translocation in adult rainbow trout (oncorhynchus mykiss) after a two-week dietary exposure. *PLoS ONE*. 15, e0239128. doi: 10.1371/journal.pone.0239128

Kirstein, I. V., Kirmizi, S., Wichels, A., Garin-Fernandez, A., Erler, R., Loder, M., et al. (2016). Dangerous hitchhikers? Evidence for potentially pathogenic vibrio spp. On microplastic particles. *Mar. Environ. Res*. 120, 1–8. doi: 10.1016/j.marenvres.2016.07.004

Koelmans, A. A., Mohamed Nor, N. H., Hermsen, E., Kooi, M., Mintenig, S. M., and De France, J. (2019). Microplastics in freshwaters and drinking water: Critical review and assessment of data quality. *Water Res*. 155, 410–422. doi: 10.1016/j.watres.2019.02.054

Kontrick, A. V. (2018). Microplastics and human health: Our great future to think about now. *J. Med. Toxicol*. 14, 117–119. doi: 10.1007/s13181-018-0661-9

Kosuth, M., Mason, S. A., and Wattenberg, E. V. (2018). Anthropogenic contamination of tap water, beer, and sea salt. *PLoS ONE*. 13, e0194970. doi: 10.1371/journal.pone.0194970

Kutralam-Muniasamy, G., Pérez-Guevara, F., Elizalde-Martínez, I., and Shruti, V. C. (2020). Branded milks – are they immune from microplastics contamination? *Sci. Total Environ*. 714, 136823. doi: 10.1016/j.scitotenv.2020.136823

Lebreton, L., Slat, B., Ferrari, F., Sainte-Rose, B., Aitken, J., Marthouse, R., et al. (2018). Evidence that the great pacific garbage patch is rapidly accumulating plastic. *Sci. Rep*. 8, 4666. doi: 10.1038/s41598-018-22939-w

Leuning, D. G., Beijer, N. R. M., du Foss,é N. A., Vermeulen, S., Lievers, E., van Kooten, C., et al. (2018). The cytokine secretion profile of mesenchymal stromal cells is determined by surface structure of the microenvironment. *Sci. Rep*. 8, 1–9. doi: 10.1038/s41598-018-25700-5

Materić, D., Kasper-Giebl, A., Kau, D., Anten, M., Greilinger, M., Ludewig, E., et al. (2020). Micro- and nanoplastics in alpine snow: A new method for chemical identification and (semi)quantification in the nanogram range. *Environ. Sci. Technol.* 54, 2353–2359. doi: 10.1021/acs.est.9b07540

Mohamed Nor, N. H., Kooi, M., Diepens, N. J., and Koelmans, A. A. (2021). Lifetime accumulation of microplastic in children and adults. *Environ Sci Technol.* 55, 5084–5096. doi: 10.1021/acs.est.0c07384

Mughini-Gras, L., van der Plaats, R. Q. J., van der Wielen, P., Bauerlein, P. S., and de Roda Husman, A. M. (2021). Riverine microplastic and microbial community compositions: A field study in the netherlands. *Water Res.* 192, 116852. doi: 10.1016/j.watres.2021.116852

Paul-Pont, I., Tallec, K., Gonzalez-Fernandez, C., Lambert, C., Vincent, D., Mazurais, D., et al. (2018). Constraints and priorities for conducting experimental exposures of marine organisms to microplastics. *Front. Mar. Sci.* 5, 1–22. doi: 10.3389/fmars.2018.00252

Rubin, A. E., Sarkar, A. K., and Zucker, I. (2021). Questioning the suitability of available microplastics models for risk assessment – a critical review. *Science of The Total Environment* 788, 147670. doi: 10.1016/j.scitotenv.2021.147670

Rubio, L., Marcos, R., and Hernandez, A. (2020). Potential adverse health effects of ingested micro- and nanoplastics on humans. Lessons learned from in vivo and in vitro mammalian models. *J. Toxicol. Environ. Health B Crit. Rev*. 23, 51–68. doi: 10.1080/10937404.2019.1700598

Schirinzi, G. F., Perez-Pomeda, I., Sanchis, J., Rossini, C., Farre, M., and Barcelo, D. (2017). Cytotoxic effects of commonly used nanomaterials and microplastics on cerebral and epithelial human cells. *Environ. Res.* 159, 579–587. doi: 10.1016/j.envres.2017.08.043

Schmid, O., and Stoeger, T. (2016). Surface area is the biologically most effective dose metric for acute nanoparticle toxicity in the lung. *J. Aerosol. Sci.* 99, 133–143. doi: 10.1016/j.jaerosci.2015.12.006

Schür, C., Rist, S., Baun, A., Mayer, P., Hartmann, N. B., and Wagner, M. (2019). When fluorescence is not a particle: The tissue translocation of microplastics in daphnia magna seems an artifact. *Environ. Toxicol. Chem.* 38, 1495–1503. doi: 10.1002/etc.4436

Schwabl, P., Köppel, S., Königshofer, P., Bucsics, T., Trauner, M., Reiberger, T., et al. (2019). Detection of various microplastics in human stool: A prospective case series. *Ann. Intern. Med.* 171, 453–457. doi: 10.7326/M19-0618

Shannon, P., Markiel, A., Ozier, O., Baliga, N. S., Wang, J. T., Ramage, D., et al. (2003). Cytoscape: A software environment for integrated models of biomolecular interaction networks. *Genome Res.* 13, 2498–2504. doi: 10.1101/gr.1239303

Shruti, V. C., Pérez-Guevara, F., Elizalde-Martínez, I., and Kutralam-Muniasamy, G. (2020). First study of its kind on the microplastic contamination of soft drinks, cold tea and energy drinks - future research and environmental considerations. *Sci Total Enviro.* 726, 138580. doi: 10.1016/j.scitotenv.2020.138580

Stock, V., Bohmert, L., Lisicki, E., Block, R., Cara-Carmona, J., Pack, L. K., et al. (2019). Uptake and effects of orally ingested polystyrene microplastic particles in vitro and in vivo. *Arch. Toxicol.* 93, 1817–1833. doi: 10.1007/s00204-019-02478-7

Stock, V., Laurisch, C., Franke, J., Dönmez, M. H., Voss, L., Böhmert, L., et al. (2021). Uptake and cellular effects of pe, pp, pet and pvc microplastic particles. *Toxicol. In Vitro.* 70, 105021. doi: 10.1016/j.tiv.2020.105021

Ter Halle, A., Jeanneau, L., Martignac, M., Jard,é E., Pedrono, B., Brach, L., et al. (2017). Nanoplastic in the north atlantic subtropical gyre. *Environ. Sci. Technol.* 51, 13689–13697. doi: 10.1021/acs.est.7b03667

USEPA. (2012). "Benchmark Dose Technical Guidance" in *Risk Assessment Forum*. Washington, DC:U.S. Environmental Protection Agency.

Vaksmaa, A., Knittel, K., Abdala Asbun, A., Goudriaan, M., Ellrott, A., Witte, H. J., et al. (2021). Microbial communities on plastic polymers in the mediterranean sea. *Front. Microbiol.* 12, 673553. doi: 10.3389/fmicb.2021.673553

Vasconcelos, D. M., Ribeiro-da-Silva, M., Mateus, A., Alves, C. J., Machado, G. C., Machado-Santos, J., et al. (2016). Immune response and innervation signatures in aseptic hip implant loosening. *J. Transl. Med.* 14, 205. doi: 10.1186/s12967-016-0950-5

Vassey, M. J., Figueredo, G. P., Scurr, D. J., Vasilevich, A. S., Vermeulen, S., Carlier, A., et al. (2020). Immune modulation by design: Using topography to control human monocyte attachment and macrophage differentiation. *Adv. Sci.* 7, 1903392. doi: 10.1002/advs.201903392

Vethaak, A. D., and Legler, J. (2021). Microplastics and human health. *Science*. 371, 672–674. doi: 10.1126/science.abe5041

Wagner, M., and Lambert, S. (2018). *Freshwater Microplastics: Emerging Environmental Contaminants*. Cham: Springer.

Wagner, S., and Reemtsma, T. (2019). Things we know and don't know about nanoplastic in the environment. *Nat. Nanotechnol.* 14, 300–301. doi: 10.1038/s41565-019-0424-z

Wayman, C., and Niemann, H. (2021). The fate of plastic in the ocean environment – a minireview. *Enviro.n Sci. Processes Impacts*. 23, 198–212. doi: 10.1039/D0EM00446D

Weber, A., Schwiebs, A., Solhaug, H., Stenvik, J., Nilsen, A. M., Wagner, M., et al. (2022). Nanoplastics affect the inflammatory cytokine release by primary human monocytes and dendritic cells. *Environ. Int.* 163, 107173. doi: 10.1016/j.envint.2022.107173

Wooley, P. H., Morrena, R., Andarya, J., Suda, S., Yanga, S. Y., Maytona, L., et al. (2002). Inflammatory responses to orthopaedic biomaterials in the murine air pouch. *Biomaterials.* 23, 517–526, doi: 10.1016/S0142-9612(01)00134-X

Wright, S. L., and Kelly, F. J. (2017). Plastic and human health: a micro issue? *Environ. Sci. Technol.* 51, 6634–6647. doi: 10.1021/acs.est.7b00423

Yong, C. Q. Y., Valiyaveetill, S., and Tang, B. L. (2020). Toxicity of microplastics and nanoplastics in mammalian systems. *Int. J. Environ. Res. Public Health.* 17, 1509. doi: 10.3390/ijerph17051509

Zettler, E. R., Mincer, T. J., and Amaral-Zettler, L. A. (2013). Life in the "plastisphere": Microbial communities on plastic marine debris. *Environ. Sci. Technol.* 47, 7137–7146. doi: 10.1021/es401288x

Zhang, N., Li, Y. B., He, H. R., Zhang, J. F., and Ma, G. S. (2021). You are what you eat: Microplastics in the feces of young men living in beijing. *Sci. Total Environ.* 767, 144345. doi: 10.1016/j.scitotenv.2020.144345

Conflict of Interest: RV and HJ were employed by SyMO-Chem B.V.

The remaining authors declare that the research was conducted in the absence of any commercial or financial relationships that could be construed as a potential conflict of interest.

Publisher's Note: All claims expressed in this article are solely those of the authors and do not necessarily represent those of their affiliated organizations, or those of the publisher, the editors and the reviewers. Any product that may be evaluated in this article, or claim that may be made by its manufacturer, is not guaranteed or endorsed by the publisher.